



Title	Characteristics, seasonality and sources of inorganic ions and trace metals in North-east Asian aerosols
Author(s)	Pavuluri, Chandra Mouli; Kawamura, Kimitaka; Mihalopoulos, Nikolaos; Fu, Pingqing
Citation	Environmental chemistry, 12(3), 338-349 <a href="https://doi.org/10.1071/EN14186">https://doi.org/10.1071/EN14186</a>
Issue Date	2015-04-20
Doc URL	<a href="http://hdl.handle.net/2115/59812">http://hdl.handle.net/2115/59812</a>
Type	article (author version)
File Information	Original (final) MS_Pavuluri et al_ Environ. Chem.- 2015, 12, 338-349.pdf



[Instructions for use](#)

1 **Characteristics, seasonality and sources of inorganic ions and trace metals**  
2 **in Northeast Asian aerosols**

3  
4 **Chandra Mouli Pavuluri<sup>A,\*</sup>, Kimitaka Kawamura<sup>A</sup>, Nikolaos Mihalopoulos<sup>A,B,C</sup> and**  
5 **PingQing Fu<sup>A,D</sup>**

6  
7 <sup>A</sup>Institute of Low Temperature Science, Hokkaido University, N19, W8, Kita-ku, Sapporo  
8 060-0819, Japan.

9 <sup>B</sup>Environmental Chemical Processes Laboratory, Department of Chemistry, University of  
10 Crete, P.O. Box 2208, 71003 Voutes, Heraklion, Greece.

11 <sup>C</sup>Present address: Institute for Environmental Research and Sustainable Development,  
12 National Observatory of Athens, GR-15236 Palea Penteli, Greece.

13 <sup>D</sup>Present address: State Key Laboratory of Atmospheric Boundary Layer Physics and  
14 Atmospheric Chemistry, Institute of Atmospheric Physics, Chinese Academy of Sciences,  
15 Beijing 100029, China.

16

17 Corresponding author. Tel.: +81 11 706 6883; fax: +81 11 706 7142. *E-mail address:*

18 [cmpavuluri@pop.lowtem.hokudai.ac.jp](mailto:cmpavuluri@pop.lowtem.hokudai.ac.jp) (C. M. Pavuluri)

19 **Environmental context.** Atmospheric aerosols impact the Earth's climate system and cause  
20 adverse effects on human health, depending on their loading and chemical composition. This  
21 study presents the chemical characteristics and seasonality of inorganic ions and trace metals  
22 in atmospheric aerosols from Sapporo, northern Japan and explores their possible sources  
23 including the potential biological sources and secondary formation processes depending on  
24 seasons over Northeast Asia. This work is relevant for atmospheric composition and climate  
25 change.

26 **Abstract.** To better understand the characteristics, seasonality and sources of inorganic  
27 aerosols in Northeast Asia, we studied total suspended particulate samples collected in  
28 Sapporo, northern Japan for inorganic ions and trace metals over one-year period.  $\text{SO}_4^{2-}$  was  
29 found as the most abundant ionic species, which accounted for on average  $43\pm 15\%$  of the  
30 measured total ionic mass followed by  $\text{Cl}^- \approx \text{NO}_3^- \approx \text{Na}^+$ . Among the metals determined, Ca was  
31 found as the most abundant ( $45\pm 5.2\%$  of the measured total metals) followed by Fe.  
32 Temporal variations of methanesulfonate ( $\text{MS}^-$ ) and  $\text{SO}_4^{2-}$  showed a clear seasonal pattern  
33 with maximum in summer followed by spring.  $\text{Cl}^-$ ,  $\text{NO}_3^-$ ,  $\text{NH}_4^+$  and  $\text{K}^+$  showed increasing  
34 trends from mid autumn to winter.  $\text{Na}^+$ ,  $\text{Ca}^{2+}$  and  $\text{Mg}^{2+}$  and crustal metals (Al, Ca, Fe, Ti and  
35 Mn) peaked in early spring.  $\text{Na}^+$  and  $\text{Mg}^{2+}$  and Ni, Cu and As were abundant in autumn  
36 whereas Zn in spring. However, Cd and Pb did not show any seasonality. Based on  
37 comparisons of such seasonal trends with those of organic tracers as well as the air mass  
38 trajectories, we infer that the seasonality in inorganic aerosols in the northeast Asian  
39 atmosphere is mainly controlled by their season-specific source(s): soil dust in early spring,  
40 biogenic emissions in spring/summer, microbial activities in autumn and forest fires/biomass  
41 burning in autumn/winter. However, contributions from anthropogenic sources are significant  
42 in all seasons. This study also suggests that fungal spores partly contribute to some trace  
43 metals (i.e., Ni, Cu, As) while pollen contributes to Zn in aerosols.

## 44 **Introduction**

45 Atmospheric aerosols have an impact on the Earth's climate system directly by absorbing and  
46 reflecting solar radiation and indirectly by acting as cloud condensation nuclei (CCN) on  
47 local, regional and global scales.<sup>[1]</sup> They also have an adverse effect on human health<sup>[2]</sup>. Such  
48 impacts of aerosols are largely depend on aerosol loading and chemical composition that are  
49 spatially and seasonally variable in the lower atmosphere<sup>[3]</sup>. Aerosol loading varies in the  
50 range of 1-100  $\mu\text{g m}^{-3}$  and dominant chemical components of the aerosols are characterized  
51 by sulfate, nitrate, ammonium, sea salt, minerals, organics and elemental carbon, each of  
52 which typically contribute about 10-30% of the overall mass load.<sup>[3]</sup> On the other hand, trace  
53 metals are typically present in elevated concentrations, especially in urban aerosols, and their  
54 water-soluble contents are significant in atmospheric waters (e.g., cloud water).<sup>[4-6]</sup>

55 Aerosol  $\text{SO}_4^{2-}$  affects the radiation budget directly by reflecting solar radiation and  
56 indirectly by altering the physical properties of aerosols.<sup>[7]</sup> Inorganic salts are more  
57 water-soluble and their solubility is much higher than organics, enhancing CCN activity of  
58 the particles.<sup>[8]</sup> Mineral dust adds complexity, because it can play a significant role in  
59 radiative forcing.<sup>[9]</sup> Trace metals play an important role in the risk of human health due to  
60 their high bioreactivity.<sup>[10,11]</sup> The water-soluble contents of trace metals can play a pivotal  
61 role in atmospheric chemistry through metal-catalyzed chemical reactions in atmospheric  
62 waters.<sup>[12,13]</sup> Furthermore, long-range atmospheric transport and dry and wet deposition of  
63 trace metals can affect the ecosystem over continental and oceanic regions because of their  
64 biogeochemical accumulation and ecological toxicity.<sup>[14,15]</sup>

65 High aerosol loadings are commonly observed in East Asia and have been attributed to  
66 anthropogenic activities.<sup>[16,17]</sup> East Asian aerosols, including dusts from arid regions in  
67 Mongolia and North China, could be further transported across the Pacific Ocean<sup>[18,19]</sup> with  
68 an impact on the regional to global climate. Radiative forcing and climatic effects over East

69 Asia have been shown to be large.<sup>[20,21]</sup> However, the aerosol chemical characteristics,  
70 seasonal variations, and sources, which are crucial in reducing the uncertainty in modeling of  
71 the aerosol impacts, are still far from being fully understood in East Asia. For example,  
72 Huang et al.<sup>[21]</sup> reported an underestimation of the annual averaged model-simulated aerosol  
73 optical depth (AOD) by ~45%. They interpreted that the obtained negative intercept is due to  
74 the inclusion of only the anthropogenic aerosols (SO<sub>4</sub><sup>2-</sup>, black carbon and organic carbon),  
75 suggesting that the contributions from natural sources might also be significant in this region.

76 Sapporo is located in the west of Hokkaido Island, northern Japan (43.07°N, 141.36°E)  
77 and is an ideal site for the study of air masses delivered from Siberia, North China, and  
78 surrounding oceans.<sup>[22]</sup> Previous studies of Sapporo aerosols demonstrated that the spring  
79 and/or summer aerosols are largely influenced by the outflows from East Asia and Siberia  
80 and are characterized by anthropogenic and biogenic (including biomass burning)  
81 contributions with the atmospheric processing during long-range transport.<sup>[22-24]</sup> However, the  
82 seasonality of various source contributions is not clearly understood due to the lack of  
83 year-round observations. To the best of our knowledge, no study has been conducted for trace  
84 metal composition of aerosols from Northeast Asia.

85 Here, we present the chemical characteristics and seasonal variations of ionic species  
86 and trace metals in the total suspended particulate matter (TSP) collected from Sapporo,  
87 northern Japan over one-year period (2009-2010). Based on seasonal enrichment of selected  
88 ionic and metal species together with the backward air mass trajectories, we infer the possible  
89 season-specific sources of inorganic aerosols over Northeast Asian region. We also discuss  
90 the role of meteorology on the seasonality. Further, based on comparisons and linear relations  
91 of selected ionic species and trace metals with organic tracers,<sup>[25]</sup> we discuss potential  
92 contributions from terrestrial biological sources to inorganic aerosols in this region.

93

## 94 **Materials and Methods**

### 95 *Aerosol sampling*

96 Aerosol (TSP) sampling ( $n = 21$ ) was performed from 2 September 2009 to 5 October 2010  
97 on the rooftop (ca. 20 m above the ground level (AGL)) of the Institute of Low Temperature  
98 Science (ILTS) building, Hokkaido University, Sapporo, northern Japan using a  
99 pre-combusted (450°C, 4 h) quartz fiber filter and high-volume air sampler ( $\sim 65 \text{ m}^3 \text{ h}^{-1}$ ). The  
100 geographical details of the sampling site has been described elsewhere.<sup>[25]</sup> Each sample was  
101 collected for ca. 2 consecutive weeks, in order to obtain sufficient amount of carbon content  
102 for radiocarbon ( $^{14}\text{C}$ ) analysis of organic molecular species, another objective of this research.  
103 Filter samples were placed in a pre-combusted glass jar with a Teflon-lined screw cap  
104 separately and stored in dark room at  $-20^\circ\text{C}$  prior to analysis.

105 It should be noted that aerosol samples collected on quartz fiber filters might have  
106 positive and negative sampling artifacts in the measurement of inorganic ions, in particular  
107  $\text{Cl}^-$ ,  $\text{NO}_3^-$  and  $\text{NH}_4^+$ .<sup>[26]</sup> In this study, the evaporative loss from the particles should be more  
108 significant than the adsorbed gases on quartz fiber filter for longer time of sampling and thus  
109 the reported concentrations may be underestimated. However, we consider that the negative  
110 bias should be minimal because the ambient temperatures encountered in Sapporo are very  
111 low even in summer (see Fig. 1) that would not cause a significant evaporative loss of  
112 ions.<sup>[26]</sup>

113

### 114 *Chemical analyses*

#### 115 *Inorganic ions*

116 Inorganic ions were measured using ion chromatograph (761 Compact IC, Metrohm,  
117 Switzerland). An aliquot of filter (1.2 cm in diameter disc) was extracted with 10 ml Milli Q  
118 water under ultrasonication for 20 min and filtered using a syringe filter (GL Sciences

119 Chromatodisc Type A, 0.45  $\mu\text{m}$ ) and then injected into IC. For anion measurement, a column  
120 of SI-90 4E (Shodex, Showa Denko, Tokyo) equipped with a suppressor was used with an  
121 eluent of 1.8 mM  $\text{Na}_2\text{CO}_3$  + 1.7 mM  $\text{NaHCO}_3$  solution at a flow rate of 1.2  $\text{ml min}^{-1}$ . For  
122 cation analysis, we used a Metrosep C2-150 (Metrohm) column with 4 mM tartaric acid  
123 ( $\text{C}_4\text{H}_6\text{O}_6$ ) + 1 mM dipicolinic acid ( $\text{C}_7\text{H}_5\text{NO}_4$ ) solution with a flow rate of 1.0  $\text{ml min}^{-1}$ . A  
124 calibration curve was evaluated by the analyses of a set of authentic standards along with a  
125 sequence of filter samples. The analytical errors in duplicate analysis of filter samples were  
126 within 14% for  $\text{MS}^-$  and 4% for other ions. The concentrations reported here are corrected for  
127 four field blanks that were collected every season.

128

#### 129 *Trace metals*

130 Trace metals were measured using an inductively coupled plasma mass spectrometry  
131 (ICP-MS, Thermo Electron X Series) after the acid microwave digestion of samples as  
132 reported by Theodosi et al.<sup>[27]</sup> Briefly, a filter disc (1.0 cm in diameter) was placed in Teflon  
133 vessel (DAP-60 K, 60 ml/40 bar), to which concentrated nitric acid was added and then  
134 digested using a microwave digestion system (Berghof MWS-2). Indium (CPI International,  
135 S4400-1000241) was used as internal standard, and a calibration curve was evaluated using  
136 standard certified solutions (CPI International). Recoveries obtained with the use of certified  
137 reference materials ranged from 90.0 to 104.1%. The concentrations reported here are not  
138 corrected for field blanks because none of the trace metals measured were found to be  
139 significant in the field blanks.

140

#### 141 *Organic tracers*

142 Details of the procedure for the determination of organic tracer compounds are  
143 described elsewhere.<sup>[25,28]</sup> Briefly, organic tracer compounds were extracted with



144 dichloromethane/methanol (2:1; v/v) under ultrasonication and derivatized with 50  $\mu$ l of  
145 N,O-bis-(trimethylsilyl)trifluoroacetamide (BSTFA) with 1% trimethylsilyl chloride and 10  
146  $\mu$ l of pyridine. The tracer compounds were then measured using a capillary gas  
147 chromatograph (Hewlett-Packard 6890) coupled to a mass spectrometer (Hewlett-Packard  
148 5973) (GC/MS).

149

### 150 *Meteorology in Sapporo*

151 24 h averaged meteorological data were obtained from Japan Meteorological Agency  
152 (<http://www.data.jma.go.jp>). The meteorological station of Sapporo is located ca. 2 km south  
153 of the sampling point. Averaged ambient temperature, relative humidity (RH), wind speed  
154 and precipitation for each sample period are presented in Fig. 1. During our campaign, the  
155 temperature, RH and wind speed ranged from -3.30  $^{\circ}$ C to 24.5  $^{\circ}$ C, 59.7-80.3% and 2.4-4.8 m  
156  $s^{-1}$ , respectively, whereas the precipitation occurred occasionally with the highest amount  
157 (range 5.5-153 mm) in summer (June to August) during rainy season with the highest  
158 frequency (range 14.3-73.3%) in winter (December-February) during snowfall season.  
159 September to November and March-May are classified as autumn and spring, respectively.  
160 The ground surfaces in Sapporo are covered with snow from late December to early April.

161

## 162 **Results and Discussion**

### 163 *Source regions of Sapporo aerosols*

164 As shown in Fig. 2, 10-day backward air mass trajectories arriving in Sapporo at 500 m AGL,  
165 which computed for every 48 h during each sample period using HYSPLIT model,<sup>[29]</sup>  
166 originated from Siberia passing over Northeast Asia and the Sea of Japan during autumn,  
167 winter and spring whereas in summer they mostly originated from the East China Sea and/or  
168 western North Pacific passing over coastal region and/or the mainland of Japan.<sup>[25]</sup> The air

169 parcels were mostly travelled at lower than 2000 m AGL in all seasons (Fig. 2) and hence,  
170 their advection from distant source regions to the receptor site should be significant.

171 As discussed in a later section (*seasonal variations*), the temporal variations of crustal  
172 metals (e.g.,  $\text{Ca}^{2+}$ , Ca, Al and Fe) showed a peak in early spring (Fig. 3), indicating a  
173 significant long-range transport of Asian dust from arid regions in Mongolia and China. On  
174 the other hand, Pavuluri et al.<sup>[25]</sup> reported that the percent modern carbon (pMC) of total  
175 carbon and water-soluble organic carbon in Sapporo aerosols started to increase from mid to  
176 late winter toward spring, although the growing season starts in May in Hokkaido when daily  
177 average temperatures are  $\geq 10^\circ\text{C}$ .<sup>[30]</sup> They interpreted such earlier increase in pMC for the  
178 long-range atmospheric transport from Eurasia. Recently, Yamamoto and Kawamura<sup>[31]</sup>  
179 reported that the terrestrial biomarkers are likely transported from Siberia, Russian Far East  
180 and Northeast China to northern Japan in winter, based on stable carbon ( $\delta^{13}\text{C}$ ) and hydrogen  
181 isotope ratios of the biomarkers detected in Sapporo snow samples together with the air mass  
182 trajectories.

183 Further based on molecular distributions of dicarboxylic acids and their  $\delta^{13}\text{C}$  in  
184 Sapporo aerosol samples collected during spring and summer as well as the air mass  
185 trajectories, Aggarwal and Kawamura<sup>[32]</sup> reported that the Sapporo aerosols are mainly  
186 influenced by the photochemically processed air masses transported from distant source  
187 regions over Northeast Asia and surrounding oceans rather than local processes. Therefore, it  
188 is very likely that the characteristics, seasonality and sources of Sapporo aerosols should  
189 reflect the regional scenario, although we do not preclude a minor impact from the sources at  
190 local scale. It should also be noted that the air masses arrived in Sapporo during each sample  
191 period (~2 week) were mostly originated from the same source region (Fig. 2), suggesting  
192 that each sample might have been influenced by only the limited source regions, despite the  
193 long sampling interval.

194

195 *Chemical characteristics*

196 Statistical summaries of ionic species (methanesulfonate:  $\text{MS}^-$  ( $\text{CH}_3\text{SO}_3^-$ ),  $\text{Cl}^-$ ,  $\text{NO}_3^-$ ,  $\text{SO}_4^{2-}$ ,  
197  $\text{Na}^+$ ,  $\text{NH}_4^+$ ,  $\text{K}^+$ ,  $\text{Ca}^{2+}$  and  $\text{Mg}^{2+}$ ) and trace metals (Al, Ca, Ti, V, Cr, Mn, Fe, Ni, Cu, Zn, As,  
198 Cd and Pb) measured in TSP samples ( $n = 21$ ) in this study are presented in Table 1. TSP  
199 masses, which were gravimetrically measured, ranged from  $13.5 \mu\text{g m}^{-3}$  to  $73.8 \mu\text{g m}^{-3}$  with  
200 an average of  $30.0 \pm 12.7 \mu\text{g m}^{-3}$ .

201

202 *Ionic species*

203  $\text{SO}_4^{2-}$  was found as the most abundant ionic species throughout the campaign ( $n = 21$ ),  
204 ranging from 1560 to 5710  $\text{ng m}^{-3}$  and accounting for on average  $43 \pm 15\%$  of the measured  
205 total ionic mass followed by  $\text{Cl}^- > \text{Na}^+ > \text{NO}_3^- > \text{Ca}^{2+} > \text{NH}_4^+$ ,  $> \text{Mg}^{2+} > \text{K}^+ > \text{MS}^-$  in autumn,  
206  $\text{Cl}^-$ ,  $\text{NO}_3^-$ ,  $\text{NH}_4^+$ ,  $\text{Na}^+$ ,  $\text{Ca}^{2+}$ ,  $\text{K}^+$ ,  $\text{Mg}^{2+}$  and  $\text{MS}^-$  in winter,  $\text{NO}_3^-$ ,  $\text{Cl}^-$ ,  $\text{Na}^+$ ,  $\text{Ca}^{2+}$ ,  $\text{NH}_4^+$ ,  $\text{Mg}^{2+}$ ,  
207  $\text{K}^+$  and  $\text{MS}^-$  in spring and  $\text{NH}_4^+$ ,  $\text{Na}^+$ ,  $\text{Ca}^{2+}$ ,  $\text{NO}_3^-$ ,  $\text{K}^+$ ,  $\text{Mg}^{2+}$ ,  $\text{MS}^-$  and  $\text{Cl}^-$  in summer (Fig. 4).  
208 However,  $\text{Cl}^-$ ,  $\text{NO}_3^-$  and  $\text{Na}^+$  were found as the second most abundant group ( $\sim 13\%$  each)  
209 followed by  $\text{NH}_4^+$ ,  $\text{Ca}^{2+}$ ,  $\text{Mg}^{2+}$ ,  $\text{K}^+$  and  $\text{MS}^-$  during the study period ( $n = 21$ ). It is noteworthy  
210 that the mass fraction of sum of inorganic ions in TSP ranged from 20% to 51% with an  
211 average of  $31 \pm 10\%$ , in which  $\text{SO}_4^{2-}$  accounted for  $12 \pm 3.8\%$ . The overall slope of linear  
212 regression line for measured total cations equivalents and anions equivalents is  $0.83 \pm 0.03$ ,  
213 although the slope value is slightly lower ( $0.67 \pm 0.07$ ) in autumn, and the correlation  
214 coefficient ( $r^2$ ) is  $> 0.95$  in each season. The deviation of the slope from 1:1 may be caused by  
215 a lack of measurements of  $\text{HCO}_3^-$ ,  $\text{PO}_4^{3-}$  and organic acid anions. These results and  
216 comparisons indicate that the ion data obtained in this study is reasonable, despite long  
217 sampling time.

218

219 *Trace metals*

220 Ca was found as the most abundant metal ranging from 196 ng m<sup>-3</sup> to 2920 ng m<sup>-3</sup>  
221 during the campaign (n = 21) (Table 1). Its relative abundance in all the metals detected is  
222 45±5.2% followed by Fe (27±4.5%). Al (21±3.1%) was found as the third most abundant  
223 metal followed by Zn > Ti > Mn > Ni > Pb > Cu > V > As > Cr > Cd (Table 1). The total  
224 mass of Al, Ca, Fe, Ti and Mn that mainly originate from the crust<sup>[33]</sup> accounted for 95±2%  
225 of all the trace metals determined in this study. On average, they accounted for 7.45±2.09%  
226 (range 2.29-10.6%) of TSP. The amount of dust estimated from Al, whose mass ratio relative  
227 to the Asian dust is 7%,<sup>[34]</sup> accounted on average for 24±8% (range 7-36%) of TSP. On the  
228 other hand, Ca concentrations obtained from ICP-MS measurements were always higher than  
229 water-soluble Ca<sup>2+</sup> obtained from IC measurements by a factor of 1.3-3.2 (Table 1). The  
230 insoluble fraction accounted for 26-69% (average 51±11%) of total Ca, which may be  
231 attributed to the existence of insoluble minerals of Ca such as calcium oxide and feldspar.  
232 However, the association of such insoluble minerals either with fine particles or coarse  
233 particles is not clear from this study.

234

235 *Seasonal variations: Possible sources and long-range atmospheric transport*

236 *MS<sup>-</sup>, SO<sub>4</sub><sup>2-</sup> and NO<sub>3</sub><sup>-</sup>: Anthropogenic and/or biogenic origins and secondary formation*  
237 *processes*

238 Seasonal variations of MS<sup>-</sup>, a tracer for biologically derived sulfur,<sup>[35]</sup> and SO<sub>4</sub><sup>2-</sup> are  
239 both characterized by a gradual increase from winter to growing season (mid spring to mid  
240 summer) by a factor of about 3 and 2, respectively, followed by a gradual decrease, although  
241 the trend is not clear in autumn (Fig. 3a). Further the MS<sup>-</sup> and SO<sub>4</sub><sup>2-</sup> were abundant in  
242 summer followed by spring (Fig. 5a). In addition, SO<sub>4</sub><sup>2-</sup> showed a linear relationship with  
243 MS<sup>-</sup> with a moderate correlation (r<sup>2</sup>=0.50) during the campaign (n = 21). The air parcels

244 arriving over Sapporo during autumn to spring originated from Siberia passing over  
245 Northeast Asia and the Sea of Japan (Fig. 2), which should have been enriched with SO<sub>2</sub>, a  
246 precursor for SO<sub>4</sub><sup>2-</sup>, emitted from biomass burning and anthropogenic activities. In addition,  
247 they should have also been enriched with dimethyl sulfide (DMS), a precursor for both MS<sup>-</sup>  
248 and SO<sub>4</sub><sup>2-</sup>, whose emission from terrestrial higher plants (e.g., 0.42 pmol m<sup>-2</sup> s<sup>-1</sup> from  
249 *Platanus orientalis* L. on a single leaf area basis)<sup>[36]</sup>, soil in forests (0.46±0.30 pmol m<sup>-2</sup> s<sup>-1</sup> to  
250 1.27±1.40 pmol m<sup>-2</sup> s<sup>-1</sup>, depending on forest type)<sup>[37]</sup> and phytoplankton bloom in the ocean<sup>[35]</sup>  
251 is significant and enhanced with increasing ambient (and soil) temperatures. In summer, the  
252 air masses originated from oceanic regions passing over coastal region and/or the mainland of  
253 Japan in summer (Fig. 2) should have mainly enriched with DMS rather than SO<sub>2</sub>.

254 In addition, ambient temperature, which promotes the photochemistry, showed a  
255 distinct seasonal trend in Sapporo with winter minima and summer maxima whereas the RH,  
256 which enhances the secondary processing of aerosols, showed a gradual increase from mid  
257 spring to late summer (Fig. 1). In contrast, precipitation that causes the wet scavenging of  
258 aerosols was relatively stable throughout the year, except in winter (high frequency) and  
259 summer (high amount) (Fig. 1). A similar pattern should prevail in Northeast Asia. Therefore,  
260 it is likely that the seasonal pattern of MS<sup>-</sup> and SO<sub>4</sub><sup>2-</sup> might have been driven mainly by  
261 enhanced emissions of their precursors from season-specific (source(s), potentially biogenic  
262 emissions in growing season, followed by intensive secondary formation processes whereas a  
263 potential removal by wet scavenging could have played a minor role.

264 Interestingly, the temporal trends of sum of hopanes (C<sub>27</sub>-C<sub>32</sub> hopanoid hydrocarbons),  
265 specific biomarkers of petroleum and coal<sup>[38]</sup> and elemental carbon that derives from fossil  
266 fuel combustion and biomass burning did not follow clear seasonal pattern during the  
267 campaign, except relatively high levels during late autumn to mid winter (Fig. 6), suggesting  
268 that the contributions from fossil fuel combustion to Sapporo aerosols are significant in all

269 seasons. Their high abundance during November to January (Fig. 6) is apparent because of  
270 increased consumption of fossil fuels in winter than in other seasons in East Asia<sup>[39]</sup>. On the  
271 contrary, sums of lipid class compounds such as fatty acids (C<sub>12</sub>-C<sub>32</sub>) and fatty alcohols  
272 (C<sub>18</sub>-C<sub>32</sub>) present clear seasonal pattern with maxima in growing season. Their averaged  
273 molecular distributions are characterized by even-carbon-numbered predominance with a  
274 maximum at C<sub>16</sub>, and C<sub>26</sub>, respectively, suggesting that they were most likely derived from  
275 terrestrial higher plant waxes.(ref) In addition, tracers of biogenic secondary organic aerosols:  
276 sums of isoprene- and  $\alpha$ -pinene-derived compounds and  $\beta$ -caryophyllenic acid, showed a  
277 clear seasonal pattern with maxima in spring to summer (Fig. 6), indicating that the  
278 contributions from biogenic emissions and subsequent secondary formation processes are  
279 significant in spring and summer.

280 In fact, the concentration range of MS<sup>-</sup> in Sapporo aerosols (Table 1) is comparable to  
281 that reported for the marine aerosols from the North Yellow Sea (12-75 ng m<sup>-3</sup>),<sup>[40]</sup> the Oki  
282 Islands in the Sea of Japan (3-95 ng m<sup>-3</sup>)<sup>[41]</sup> and other oceanic regions (~10-100 ng m<sup>-3</sup>)<sup>[35,42]</sup>  
283 and the forest aerosols (9-95 ng m<sup>-3</sup>) collected at two levels (~2 m and ~15 m) of the  
284 experimental forest in Sapporo, Japan, where the canopy height is ~20 m.<sup>[43]</sup> The  
285 contributions of MS<sup>-</sup> in the marine and forest aerosols were attributed to the emission of  
286 DMS from phytoplankton bloom and forest floor, respectively, followed by the subsequent  
287 photochemical oxidation. It is noteworthy that the averaged seasonal variations of MS<sup>-</sup> in  
288 marine aerosols over Oki Islands in the Sea of Japan for a 9-year period showed a sharp  
289 increase from March to May followed by a gradual decrease to October.<sup>[41]</sup> In contrast, in  
290 Sapporo aerosols, MS<sup>-</sup> concentrations gradually increased from March to May and stayed  
291 high until late summer followed by a gradual decrease to autumn (Fig. 2a). The average  
292 concentration of MS<sup>-</sup> (64 ng m<sup>-3</sup>) in Sapporo summer aerosols is significantly higher than that  
293 (39 ng m<sup>-3</sup>) reported in 2006 summer aerosols (July-August) from the North Yellow Sea.

294 In addition, the molar ratios of  $\text{MS}^-$  to  $\text{SO}_4^{2-}$ , which can be used as an indicator of the  
295 relative contributions of the  $\text{SO}_4^{2-}$  derived from biogenic DMS and anthropogenic  $\text{SO}_2$  to  
296 measured  $\text{SO}_4^{2-}$ ,<sup>[35]</sup> in Sapporo summer aerosols (average 1.55) is three times higher than that  
297 (0.55%) of the summer aerosols from the North Yellow Sea.<sup>[40]</sup> Such differences might have  
298 occurred probably due to more continental outflow of anthropogenic emissions from China  
299 over the North Yellow Sea, compared to the Hokkaido region. Alternatively, additional  
300 contribution of  $\text{MS}^-$  originated from higher plant emissions is possible in Sapporo aerosols.  
301 Thus our results and their comparisons with organic tracers and with literature imply that the  
302 seasonality of  $\text{MS}^-$  and  $\text{SO}_4^{2-}$  in Sapporo aerosols should have been driven by the enhanced  
303 biogenic emissions of DMS and subsequent intensive secondary processes in spring and  
304 summer. On the other hand, the high frequency of precipitation should also lower the  
305 concentrations of  $\text{SO}_4^{2-}$  in winter, despite the enhanced contributions from the increased  
306 anthropogenic emissions.

307 The concentrations of  $\text{NO}_3^-$ , which is also produced by secondary processes in the  
308 atmosphere, are higher in autumn to spring and lower in summer, being different from the  
309 case of  $\text{SO}_4^{2-}$  (Fig. 2a). This discrepancy should be due to differences in mechanistic chains  
310 responsible for their formation and emission rates of their precursors, in addition to a  
311 potential loss of  $\text{NO}_3^-$  by dry deposition in summer (see next Sect.). In fact, the  $[\text{NH}_4^+]/[\text{SO}_4^{2-}]$   
312 molar ratios were  $<1.5$ , except in winter, indicating the  $\text{NH}_4^+$ -poor atmosphere<sup>[26]</sup> during the  
313 campaign. Under such conditions, the production of  $(\text{NH}_4)_2\text{SO}_4$  is favored over the formation  
314 of  $\text{NH}_4\text{NO}_3$  through the homogeneous reaction between  $\text{H}_2\text{SO}_4$  and  $\text{NH}_3$ , which is intensive  
315 under high temperature and RH, rather than  $\text{HNO}_3$  and  $\text{NH}_3$ . Meanwhile,  $\text{HNO}_3$  is more  
316 likely reacted with sea-salt (e.g.,  $\text{NaCl}$ ) and crustal particles (e.g.,  $\text{CaCO}_3$ ).<sup>[26]</sup>

317 On the other hand, the origins of the air parcels that arrived in Sapporo in each season  
318 may have also influenced the different seasonality between  $\text{SO}_4^{2-}$  and  $\text{NO}_3^-$ . The air masses

319 that originated from Siberia passing over Northeast Asia during autumn to spring (Fig. 2)  
320 should have been enriched with  $\text{NO}_x$  (the precursors of  $\text{NO}_3^-$ ) and  $\text{SO}_2$  that are emitted from  
321 biomass burning and anthropogenic activities. In addition, the air masses may be enriched  
322 with DMS emitted from terrestrial vegetation in spring. In summer, the air masses originating  
323 from oceanic regions passing over coastal region and/or the mainland of Japan (Fig. 2) should  
324 contain abundant DMS emitted from both phytoplankton bloom and terrestrial higher plants  
325 rather than  $\text{NO}_x$  and  $\text{SO}_2$ . Furthermore, it is likely that  $\text{SO}_4^{2-}$  is associated with fine particles  
326 whereas  $\text{NO}_3^-$  with coarse particles, and hence during long-range transport  $\text{SO}_4^{2-}$  should  
327 become more abundant than  $\text{NO}_3^-$  due to a preferential deposition of coarse particles over  
328 fine particles in summer (see the following sect.).

329

330  *$\text{Cl}^-$ ,  $\text{Na}^+$ ,  $\text{Mg}^{2+}$  and  $\text{Ca}^{2+}$ : Emissions from natural sources including microbial activities*

331 Concentrations of  $\text{Cl}^-$  are higher in autumn to spring than in summer whereas  $\text{Na}^+$  and  
332  $\text{Mg}^{2+}$  peaked in autumn and early spring and minimized in winter as well as in summer (Fig.  
333 3a). Those of  $\text{Ca}^{2+}$  stayed low in autumn and summer and slightly decreased in winter,  
334 however, they showed a peak in early spring (Fig. 3a).  $\text{Cl}^-$  and  $\text{Na}^+$  are considered as typical  
335 components of sea-salt whereas  $\text{Mg}^{2+}$  and  $\text{Ca}^{2+}$  are crustal components. The higher  
336 concentrations of  $\text{Mg}^{2+}$  and  $\text{Na}^+$  in autumn may be attributable to significant mixing of soil  
337 dust and sea-salt when the air masses passed over Northeast Asia and the Sea of Japan. On  
338 the contrary, the concentrations of  $\text{Ca}^{2+}$  and  $\text{Cl}^-$  in autumn were almost similar to those in  
339 winter (Fig. 3a), suggesting that  $\text{Mg}^{2+}$  and  $\text{Na}^+$  are derived from other source(s) rather than  
340 soil dust and sea-salt in this season.

341 It is noteworthy that  $\text{Na}^+$  is most abundant in autumn (Fig. 5b), although its peak values  
342 in spring are comparable to those in autumn and the average and median values of  $\text{Mg}^{2+}$  in  
343 autumn and spring are the same ( $0.19 \mu\text{g m}^{-3}$ ) (Fig. 3a), despite a significant sea-salt



344 contribution in summer, and enhanced soil dust contribution in early spring as discussed  
345 below. In addition,  $Mg^{2+}$  showed insignificant but negative relations with Al, a tracer of  
346 crustal emission,<sup>[34]</sup> in autumn ( $r^2 = 0.19$ ), suggesting that soil dust may not be a major source.  
347 As noted earlier, sea-salt contribution to  $Na^+$  may not be the major source in autumn.  
348 Therefore, it is likely that the abundant  $Mg^{2+}$  and  $Na^+$  in autumn may be derived from other  
349 source, probably microbial activities. Fungal activities in soil surface emit the spores and  
350 hyphae, which are significantly enriched with several elements including Na and Mg.<sup>[44]</sup>  
351 Their activities on fallen leaves may be increased during defoliation season. In fact, the  
352 concentration of mannitol that is mainly produced by fungi is highest in autumn ( $20.3 \pm 13.3$   
353  $ng\ m^{-3}$ ) followed by summer ( $7.07 \pm 3.38\ ng\ m^{-3}$ ) (Fig. 6).<sup>[25]</sup> Therefore, we consider that the  
354 fungal activities are the potential sources of  $Na^+$  and  $Mg^{2+}$  in autumn.

355 The relatively low concentrations of ions may be associated with wet scavenging in  
356 winter when snow precipitation frequently occurred (Fig. 1). Their peaks (e.g.,  $Ca^{2+}$ ) in early  
357 spring may be due to the soil dust injection to the atmosphere from the arid regions of  
358 Mongolia and Northeast China<sup>[34]</sup> followed by a long-range transport. In fact, two massive  
359 dust storms occurred in Mongolia and Northeast China in early spring on 20 and 31 March  
360 2010, respectively (<http://earthobservatory.nasa.gov>). Liu et al.<sup>[45]</sup> reported that the dust  
361 storm in Mongolia was blown in Beijing, China and the dust plume covered over the  
362 downwind regions including Hokkaido Island.

363 In summer, the lowest concentrations of  $Cl^-$ ,  $Na^+$ ,  $Mg^{2+}$  and  $Ca^{2+}$  as well as  $NO_3^-$ , which  
364 exist preferably in coarse mode, might be associated with the enhanced dry and wet  
365 deposition. Agarwal et al.<sup>[23]</sup> reported that the concentrations of these ions ( $Na^+$  is not  
366 reported) maximized in coarse ( $>7.0\ \mu m$  in diameter) size particles collected in summer (8-11  
367 August) 2005 from the same site. Dry deposition velocities are higher ( $1.2-5\ cm\ s^{-1}$ ) for  
368 coarse mode particles than accumulation mode particles ( $0.001-0.05\ cm\ s^{-1}$ ) and the

369 deposition rates are further influenced by surface thermal response to insolation on  
370 convective mixing in the boundary layer.<sup>[46]</sup> The high temperature and low wind speed in  
371 summer (Fig. 1) might have caused boundary layer convective instability and reduction in  
372 convective mixing of pollutants, respectively, and hence, the dry deposition of coarse  
373 particles might be intensive in summer. In addition, the washout of pollutant should be more  
374 efficient in summer due to high amount of precipitation (Fig. 1). It is known that precipitation  
375 scavenges coarse particles more efficiently than fine ones.

376

#### 377 *NH<sub>4</sub><sup>+</sup> and K<sup>+</sup>: Biomass burning emissions*

378 NH<sub>4</sub><sup>+</sup> and K<sup>+</sup> significantly increased from mid- to late-autumn and stayed high until  
379 mid winter (Fig. 2a). NH<sub>4</sub><sup>+</sup> then showed a gradual decrease toward early spring whereas K<sup>+</sup>  
380 showed a decrease toward late winter followed by an increase in early spring and thereafter.  
381 They stayed relatively stable, except for few cases, from mid spring to summer (Fig. 3a). It is  
382 well recognized that NH<sub>4</sub><sup>+</sup> and K<sup>+</sup> are mainly originate from biomass burning and biogenic  
383 emissions.<sup>[47-49]</sup> Higher levels of these species during mid autumn to mid winter may be  
384 associated with forest fires and/or biomass burning on a local and/or regional scale, whereas  
385 the increase of K<sup>+</sup> from late winter to early spring may be caused by the long-range  
386 atmospheric transport of soil dust. Concentrations of levoglucosan, an excellent tracer of  
387 biomass burning<sup>[50]</sup>, were also high in mid autumn to mid winter (Fig. 6), further supporting  
388 the enhanced contributions from the biomass burning during this period.

389 In spring and summer, the temporal trends of K<sup>+</sup> and NH<sub>4</sub><sup>+</sup> (Fig. 3a) are not consistent  
390 with that of levoglucosan (Fig. 6). This discrepancy is probably due to significant  
391 decomposition of levoglucosan<sup>[51]</sup> and (or) biogenic contributions of K<sup>+</sup> and NH<sub>4</sub><sup>+</sup> in during  
392 growing season. In fact, K<sup>+</sup> in Sapporo aerosols showed a good correlation with SO<sub>4</sub><sup>2-</sup> in  
393 spring ( $r=0.71$ ), which is partly derived from biogenic emissions. However, MODIS fire

394 detections indicated that the forest fires/biomass burning events are significant over Siberia  
395 and northeast China in spring and over Japan mainland in summer 2010 (see Fig. S1). The air  
396 masses arriving over Sapporo in spring originated in Siberia and passed over Northeast China  
397 whereas in summer, they passed over Japan mainland (Fig. 2), which should have been  
398 enriched with biomass burning emissions. Therefore, we consider that the higher levels of  
399  $\text{NH}_4^+$  and  $\text{K}^+$  from mid spring to late summer should have associated with enhanced biomass  
400 burning emissions, although we do not preclude a minor contribution from biogenic  
401 emissions.

402

403 *Trace metals: Possible contributions from soil dust injection, anthropogenic emissions*  
404 *and biological sources*

405 Crustal metals such as Al, Ca, Fe, Ti and Mn<sup>[33]</sup> did not show any significant seasonal  
406 variations, although their concentrations are relatively low in winter (Fig. 3b) probably due to  
407 wet scavenging by snowfall (Fig. 1). They showed a very sharp increase in early spring  
408 (April 1-15) followed by a gradual decrease to late autumn (Fig. 3b). Being similar to  $\text{Ca}^{2+}$ ,  
409 these trends indicate a significant contribution of soil dust particles that are transported from  
410 the arid regions in Mongolia and Northeast China,<sup>[45]</sup> as discussed earlier.

411 Ni showed a gradual decrease from autumn to mid winter and a gradual increase toward  
412 early summer followed by a decrease in mid summer (Fig. 3b). The seasonal trends of both  
413 Cu and As are quite similar to that of Ni in autumn to mid spring and the rest of the period  
414 (Fig. 3b). The concentrations of Zn are rather constant during the campaign, except for spring:  
415 a gradual increase from winter to late spring followed by a decrease to summer, although a  
416 high value was observed in early summer (Fig. 3b). V and Cr did not vary significantly in  
417 autumn but showed a gradual decrease in winter followed by a sharp increase in early spring.  
418 Thereafter V stayed relatively high until late summer whereas Cr decreased gradually toward

419 early summer (Fig. 3b). In contrast, Cd and Pb did not show any clear trend throughout the  
420 campaign (Fig. 3b).

421 The trace metals: Ni, Cu, As, Zn, V, Cr, Cd and Pb, are considered to be emitted to the  
422 atmosphere by fossil fuel combustion, metallurgical industrial activity and traffic pollution.<sup>[52]</sup>  
423 Therefore, it is likely that they originate from anthropogenic sources over the region. The  
424 lower values in winter might be associated with wet scavenging by snowfall (Fig. 1) whereas  
425 a sharp increase in early spring may be due to soil dust injection from arid regions of  
426 Mongolia and northeast China,<sup>[45]</sup> where the soil surface could have been enriched with  
427 anthropogenic pollutants. However, the reason for a gradual decrease in autumn to winter and  
428 a gradual increase from winter to late spring of some trace metals (i.e., Ni, Cu, As, Zn) is  
429 unclear. In fact, the combustion tracers; (i) hopanes<sup>[38]</sup> (ii) levoglucosan<sup>[50]</sup> and (iii) EC, did  
430 not show such seasonal trends in Sapporo aerosols.<sup>[25]</sup> Hence, it is possible that the seasonal  
431 trends of Ni, Cu, As and Zn should have been driven by other season-specific source(s).

432 Interestingly, Ni, Cu and As (Fig. 3b) showed a seasonal trend similar to that of  
433 mannitol (Fig. 5), which is considered as a tracer for bioaerosol (fungal species).<sup>[53]</sup> On the  
434 other hand, seasonal pattern of Zn (Fig. 3b) is similar to that of sucrose (Fig. 5), which is a  
435 tracer of pollens emitted from terrestrial plants.<sup>[54]</sup> Fungi uptake the trace metals from the  
436 substrate and the extent of their bioaccumulation is species-specific.<sup>[55]</sup> As shown in Fig. 7,  
437 Ni, Cu and As positively correlate with mannitol ( $r^2=0.33$ ,  $0.47$  and  $0.28$ , and  $p = 0.006$ ,  
438  $0.001$  and  $0.013$ , respectively). It is also noteworthy that these metals negligibly correlated  
439 with hopanes ( $r^2=0.22$ ,  $0.01$  and  $0.001$ ), levoglucosan ( $r^2=0.25$ ,  $0.03$  and  $0.03$ ) and EC  
440 ( $r^2=0.03$ ,  $0.08$  and  $0.18$ , respectively). On the other hand, Zn showed a positive correlation  
441 ( $r^2=0.60$ ) with sucrose whereas weak or no correlations with hopanes ( $r^2=0.24$ ), levoglucosan  
442 ( $r^2=(-)0.001$ ) and EC ( $r^2=0.12$ ) in spring, although no relation was found in other seasons. In  
443 fact, Zn is present in pollen grains.<sup>[56]</sup> Furthermore, we found that Cu and Zn, which are

444 considered to be emitted from metallurgical industrial activity,<sup>[52]</sup> are associated with  
445 different factors obtained from Varimax rotated factor analysis of trace metals (see Table 3).  
446 Therefore, we consider that the terrestrial biological sources including microbial activities  
447 should have partly contributed to trace metals in Sapporo aerosols. Nriagu<sup>[57]</sup> reported that  
448 biogenic sources could account for 30-50% of the global baseline emissions of trace metals,  
449 which again supports our assumption.

450

#### 451 *Factor analysis*

452 Factor analysis (FA), which does not require a prior information on source composition,<sup>[58]</sup>  
453 has been widely used to apportion the sources of chemical species in atmospheric aerosols.<sup>[59]</sup>  
454 In this study, Varimax rotated FA was applied to inorganic ion and trace metal data sets (n =  
455 21) to further examine the likely sources discussed in the previous section and the obtained  
456 results are presented in Tables 2 and 3, respectively. The FA resulted three factors each with  
457 Eigen values greater than 1 that explain 87% and 83% of the total variance of the data sets,  
458 respectively. The factor loadings: >0.75, 0.75-0.5 and 0.5-0.3, which can be classified as  
459 strong, moderate and weak, respectively,<sup>[60]</sup> are used to infer the factors to distinguish  
460 possible sources. It should be noted that the sample size ( $n = 30 + (V+3)/2$ ) of both ions and  
461 metals is relatively small for FA.<sup>[58]</sup> However, the communalities obtained for all species  
462 are >0.6, except for V and Zn (0.5), suggesting that the obtained results from the FA of these  
463 data sets should be reasonable.<sup>[61]</sup>

464

#### 465 *Inorganic ions*

466 The first factor, which accounted for 31% of total variance, is strongly loaded with  
467  $Mg^{2+}$  and  $Na^+$  and moderately with  $Ca^{2+}$  and weakly with  $Cl^-$  (Table 2).  $Na^+$  and  $Ca^{2+}$  are  
468 typical sea-salt and crustal components, respectively.  $Mg^{2+}$  originates mostly from soil dust

469 but oceanic emissions also could contribute at significant levels. In fact,  $Mg^{2+}$  showed a  
470 positive correlation ( $r^2 = 0.24$ ) with Al, a tracer for crustal origin,<sup>[34]</sup> during the campaign ( $n$   
471 = 21). Hence, this factor can be attributed to a natural source: soil dust and sea-salt. It is  
472 noteworthy that both  $NO_3^-$  and  $K^+$  are positively correlated with this factor, although the  
473 loading is very poor (Table 3), suggesting important heterogeneous reactions (mainly for  $NO_3^-$ )  
474 with dust and sea-salt and/or that biomass burning emissions may be associated with this  
475 factor.

476 The second factor, which accounted for 30% of total variance, strongly loaded with  
477  $MS^-$  and  $SO_4^{2-}$  (Table 2). These ions are produced in the atmosphere by secondary  
478 transformations through photochemical reactions of their precursor compounds (DMS,  $SO_2$ )  
479 of biogenic and anthropogenic/biogenic origins, respectively, as discussed earlier. Therefore  
480 it is apparent that the second factor represents the secondary aerosols produced by  
481 homogeneous photochemical reactions. A weak positive correlation of  $K^+$  and  $Ca^{2+}$  with this  
482 factor may be due to a possible association of  $SO_4^-$  with these metal ions.

483 The third factor, which accounted for 25% of total variance, is strongly associated with  
484  $NO_3^-$ ,  $NH_4^+$  and  $K^+$  and weakly with  $Cl^-$  and  $Ca^{2+}$  as well as  $SO_4^-$  (Table 2).  $NO_3^-$  and  $SO_4^-$   
485 can be derived from fossil fuel combustion and/or biomass burning emissions whereas  $NH_4^+$   
486 and  $K^+$  from biomass burning and/or biogenic emissions. Hence, this factor can mainly be  
487 interpreted as biomass burning mixed with other anthropogenic emissions but biogenic  
488 emissions may also be associated.

489

#### 490 *Trace metals*

491 The first factor is strongly loaded with Al, Ca, Ti, Mn, and Fe, which are typical crustal  
492 components<sup>[33,34]</sup> and with Cr, accounting for 41% of total variance. V is weakly loaded with  
493 this factor whereas Ni, As and Pb are also positively correlated, however, their loadings are

494 very poor (Table 3). Hence, this factor can mainly be attributed to soil dust. The second  
495 factor is strongly loaded with Ni and Cu, moderately with V and As, and weakly with Zn,  
496 accounting for 21% of total variance (Table 3). The metallurgical industrial activities have  
497 been considered as the major source of Cu, As and Zn whereas oil combustion is considered  
498 as a source of Ni and V.<sup>[52]</sup> Therefore, this factor may be associated with industrial emissions  
499 mixed with other (fossil fuel combustion) anthropogenic sources. The third factor correlates  
500 strongly with Cd and Pb, moderately with Zn and weakly with Cr and As, accounting for  
501 20% of total variance (Table 3). Mn, Fe and Cu also showed a positive correlation with this  
502 factor, although the coefficient is poor. All these trace metals are most likely derived from the  
503 anthropogenic activities, particularly fossil fuel combustion.<sup>[52]</sup> Hence, this factor can be  
504 interpreted as emissions of fossil fuel combustion and road dust from the presence of Pb, Zn,  
505 Cu and crustal elements.

506

### 507 **Summary and conclusions**

508 Atmospheric aerosol (TSP) samples collected from Sapporo, northern Japan for one-year  
509 period, were studied for inorganic ions and trace metals using ion chromatograph (IC) and  
510 inductively coupled plasma mass spectrometry (ICP-MS), respectively.  $\text{SO}_4^{2-}$  was found as  
511 the most abundant ion whereas Ca was the most abundant metal. The mass fraction of sum of  
512 inorganic ions in TSP ranged from 20% to 51% with an average of  $31 \pm 10\%$ , in which  $\text{SO}_4^{2-}$   
513 accounted for  $12 \pm 3.8\%$ . The group of crustal metals alone accounted for  $95 \pm 2\%$  of the total  
514 metals determined. The seasonal trends of  $\text{MS}^-$  (a tracer for biologically derived sulfur) and  
515  $\text{SO}_4^{2-}$  showed maxima in growing season, while crustal metals peaked in early spring,  
516 suggesting that biogenic emissions maximized in spring/summer whereas soil dust injection  
517 did in early spring.  $\text{Na}^+$  and  $\text{Mg}^{2+}$  were abundant, despite insignificant contribution of both  
518 sea-salt and soil dust, in autumn. In addition, Ni, Cu and As showed maxima in autumn. Such

519 seasonal trends and their comparison with those of tracer species reported in our samples<sup>[25]</sup>  
520 suggest the potential contribution of microbial activities in autumn.  $\text{NH}_4^+$  and  $\text{K}^+$  became  
521 more abundant from mid autumn to mid winter as well as from mid spring to late summer,  
522 indicating the enhanced contributions from biomass burning in these periods. The present  
523 results together with factor analysis of ionic species and trace metals, comparisons of the  
524 seasonality of specific ions and metals with the tracer species, and air mass trajectories, imply  
525 that the long-range atmospheric transport of soil dust, and anthropogenic emissions including  
526 biomass burning, biogenic emissions including microbial activities, and secondary production  
527 from both anthropogenic and biogenic emissions are the major sources of Northeast Asian  
528 aerosols, with the relative contributions being depending on seasons.

529

### 530 **Supplementary material**

531 Maps of monthly averages of active fires detected using MODIS data from the Terra satellite  
532 over the Asian region for the period of September 2009 and August 2010 are provided in Fig.  
533 S1. The global maps of active fire detections were obtained from MODIS Rapid Response  
534 website (<http://rapidfires.sci.gsfc.nasa.gov/>).

535

### 536 **Acknowledgements**

537 This study was in part supported by Japan Society for the Promotion of Science  
538 (Grant-in-Aid Nos. 1920405 and 24221001) and the Environment Research and Technology  
539 Development Fund (B903) of the Ministry of the Environment, Japan. The authors thank Dr.  
540 Theodosi Christina for trace metals analysis.



## References

- 541  
542
- 543 [1] V. Ramanathan, P. J. Crutzen, J. T. Kiehl, D. Rosenfeld, Aerosols, climate, and the  
544 hydrological cycle. *Science* **2001**, *294* (5549), 2119.
- 545 [2] A. Nel, Air pollution-related illness: Effects of particulates. *Science* **2005**, *308*, 804.
- 546 [3] U. Pöschl, Atmospheric aerosols: Composition, transformation, climate and health effects.  
547 *Angew. Chem. Int. Ed.* **2005**, *44*, 7520.
- 548 [4] T. Moreno, X. Querol, A. Alastuey, C. Reche, M. Cusack, F. Amato, M. Pandolfi, J. Pey,  
549 A. Richard, A. S. H. Prevot, M. Furger, W. Gibbons, Variations in time and space of trace  
550 metal aerosol concentrations in urban areas and their surroundings. *Atmos Chem Phys* **2011**,  
551 *11* (17), 9415.
- 552 [5] S. Gioia, D. Weiss, B. Coles, T. Arnold, M. Babinski, Accurate and precise zinc isotope  
553 ratio measurements in urban aerosols. *Anal Chem* **2008**, *80* (24), 9776.
- 554 [6] W. J. Li, Y. Wang, J. L. Collett, J. M. Chen, X. Y. Zhang, Z. F. Wang, W. X. Wang,  
555 Microscopic evaluation of trace metals in cloud droplets in an acid precipitation region.  
556 *Environ Sci Technol* **2013**, *47* (9), 4172.
- 557 [7] C. Deandreis, Y. Balkanski, J. L. Dufresne, A. Cozic, Radiative forcing estimates of  
558 sulfate aerosol in coupled climate-chemistry models with emphasis on the role of the  
559 temporal variability. *Atmos Chem Phys* **2012**, *12* (12), 5583.
- 560 [8] Q. Zhang, J. Meng, J. Quan, Y. Gao, D. Zhao, P. Chen, H. He, Impact of aerosol  
561 composition on cloud condensation nuclei activity. *Atmos Chem Phys* **2012**, *12* (8), 3783.
- 562 [9] F. J. Dentener, G. R. Carmichael, Y. Zhang, J. Lelieveld, P. J. Crutzen, Role of mineral  
563 aerosol as a reactive surface in the global troposphere. *J Geophys Res-Atmos* **1996**, *101* (D17),  
564 22869.
- 565 [10] F. Schaumann, P. J. A. Borm, A. Herbrich, J. Knoch, M. Pitz, R. P. F. Schins, B. Luettig,  
566 J. M. Hohlfeld, J. Heinrich, N. Krug, Metal-rich ambient particles (particulate matter(2.5))  
567 cause airway inflammation in healthy subjects. *Am J Resp Crit Care* **2004**, *170* (8), 898.
- 568 [11] S. Zahran, M. A. S. Laidlaw, S. P. McElmurry, G. M. Filippelli, M. Taylor, Linking  
569 source and effect: Resuspended soil lead, air lead, and children's blood lead levels in detroit,  
570 michigan. *Environ Sci Technol* **2013**, *47* (6), 2839.
- 571 [12] Y. G. Zuo, J. Hoigne, Photochemical decomposition of oxalic, glyoxalic and  
572 pyruvic-acid catalyzed by iron in atmospheric waters. *Atmos Environ* **1994**, *28* (7), 1231.
- 573 [13] C. M. Pavuluri, K. Kawamura, Evidence for 13-carbon enrichment in oxalic acid via  
574 iron catalyzed photolysis in aqueous phase. *Geophys Res Lett* **2012**, *39*, L03802 DOI:  
575 10.1029/2011gl050398.

- 576 [14] W. J. Li, T. Wang, S. Z. Zhou, S. C. Lee, Y. Huang, Y. Gao, W. X. Wang, Microscopic  
577 observation of metal-containing particles from chinese continental outflow observed from a  
578 non-industrial site. *Environ Sci Technol* **2013**, *47* (16), 9124.
- 579 [15] K. W. Fomba, K. Muller, D. van Pinxteren, H. Herrmann, Aerosol size-resolved trace  
580 metal composition in remote northern tropical atlantic marine environment: Case study cape  
581 verde islands. *Atmos Chem Phys* **2013**, *13* (9), 4801.
- 582 [16] G. R. Carmichael, B. Adhikary, S. Kulkarni, A. D'Allura, Y. Tang, D. Streets, Q. Zhang,  
583 T. C. Bond, V. Ramanathan, A. Jamroensan, P. Marrapu, Asian aerosols: Current and year  
584 2030 distributions and implications to human health and regional climate change. *Environ.*  
585 *Sci. Technol.* **2009**, *43* (15), 5811.
- 586 [17] L. K. Sahu, Y. Kondo, Y. Miyazaki, M. Kuwata, M. Koike, N. Takegawa, H. Tanimoto,  
587 H. Matsueda, S. C. Yoon, Y. J. Kim, Anthropogenic aerosols observed in asian continental  
588 outflow at jeju island, korea, in spring 2005. *J Geophys Res-Atmos* **2009**, *114*.
- 589 [18] K. Kawamura, M. Kobayashi, N. Tsubonuma, M. Mochida, T. Watanabe, M. Lee,  
590 Organic and inorganic compositions of marine aerosols from east asia: Seasonal variations of  
591 water-soluble dicarboxylic acids, major ions, total carbon and nitrogen, and stable c and n  
592 isotopic composition. In *Geochemical investigations in earth and space science: A tribute to*  
593 *isaac r. Kaplan*, Hill, R. J.; Leventhal, J.; Aizenshtat, Z.; Baedecker, M. J.; Claypool, G.;  
594 Eganhouse, R.; Goldhaber, M.; Peters, K., Eds. The Geochemical Society: 2004; p  
595 Publication No. 9.
- 596 [19] I. Uno, K. Eguchi, K. Yumimoto, Z. Liu, Y. Hara, N. Sugimoto, A. Shimizu, T.  
597 Takemura, Large asian dust layers continuously reached north america in april 2010. *Atmos*  
598 *Chem Phys* **2011**, *11* (14), 7333.
- 599 [20] T. Nakajima, S. C. Yoon, V. Ramanathan, G. Y. Shi, T. Takemura, A. Higurashi, T.  
600 Takamura, K. Aoki, B. J. Sohn, S. W. Kim, H. Tsuruta, N. Sugimoto, A. Shimizu, H.  
601 Tanimoto, Y. Sawa, N. H. Lin, C. T. Lee, D. Goto, N. Schutgens, Overview of the  
602 atmospheric brown cloud east asian regional experiment 2005 and a study of the aerosol  
603 direct radiative forcing in east asia. *J Geophys Res-Atmos* **2007**, *112* (D24).
- 604 [21] Y. Huang, R. E. Dickinson, W. L. Chameides, Impact of aerosol indirect effect on  
605 surface temperature over east asia. *P Natl Acad Sci USA* **2006**, *103* (12), 4371.
- 606 [22] S. G. Aggarwal, K. Kawamura, Carbonaceous and inorganic composition in long-range  
607 transported aerosols over northern japan: Implication for aging of water-soluble organic  
608 fraction. *Atmos Environ* **2009**, *43* (16), 2532.
- 609 [23] S. Agarwal, S. G. Aggarwal, K. Okuzawa, K. Kawamura, Size distributions of  
610 dicarboxylic acids, ketoacids, alpha-dicarbonyls, sugars, wsoc, oc, ec and inorganic ions in

611 atmospheric particles over northern japan: Implication for long-range transport of siberian  
612 biomass burning and east asian polluted aerosols. *Atmos Chem Phys* **2010**, *10* (13), 5839.

613 [24] C. M. Pavuluri, K. Kawamura, M. Kikuta, E. Tachibana, S. G. Aggarwal, Time-resolved  
614 variations in the distributions of inorganic ions, carbonaceous components, dicarboxylic acids  
615 and related compounds in atmospheric aerosols from sapporo, northern japan during  
616 summertime. *Atmos Environ* **2012**, *62*, 622.

617 [25] C. M. Pavuluri, K. Kawamura, M. Uchida, M. Kondo, P. Q. Fu, Enhanced modern  
618 carbon and biogenic organic tracers in northeast asian aerosols during spring/summer. *J*  
619 *Geophys Res-Atmos* **2013**, *118* (5), 2362.

620 [26] S. Squizzato, M. Masiol, A. Brunelli, S. Pistollato, E. Tarabotti, G. Rampazzo, B. Pavoni,  
621 Factors determining the formation of secondary inorganic aerosol: A case study in the po  
622 valley (italy). *Atmos Chem Phys* **2013**, *13* (4), 1927.

623 [27] C. Theodosi, Z. Markaki, A. Tselepidis, N. Mihalopoulos, The significance of  
624 atmospheric inputs of soluble and particulate major and trace metals to the eastern  
625 mediterranean seawater. *Mar Chem* **2010**, *120* (1-4), 154.

626 [28] P. Q. Fu, K. Kawamura, C. M. Pavuluri, T. Swaminathan, J. Chen, Molecular  
627 characterization of urban organic aerosol in tropical india: Contributions of primary  
628 emissions and secondary photooxidation. *Atmos Chem Phys* **2010**, *10* (6), 2663.

629 [29] R. R. Draxler, G. D. Rolph, Hysplit (hybrid single-particle lagrangian integrated  
630 trajectory) model access via noaa arl ready website. Noaa air resources laboratory, silver  
631 spring, md. [Http://ready.Arl.Noaa.Gov/hysplit.Php](http://ready.arl.noaa.gov/hysplit.php). **2012**.

632 [30] Y. Toma, F. G. Fernandez, S. Sato, M. Izumi, R. Hatano, T. Yamada, A. Nishiwaki, G.  
633 Bollero, J. R. Stewart, Carbon budget and methane and nitrous oxide emissions over the  
634 growing season in a miscanthus sinensis grassland in tomakomai, hokkaido, japan. *Gcb*  
635 *Bioenergy* **2011**, *3* (2), 116.

636 [31] S. Yamamoto, K. Kawamura, O. Seki, Long-range atmospheric transport of terrestrial  
637 biomarkers by the asian winter monsoon: Evidence from fresh snow from sapporo, northern  
638 japan. *Atmos Environ* **2011**, *45* (21), 3553.

639 [32] S. G. Aggarwal, K. Kawamura, Molecular distributions and stable carbon isotopic  
640 compositions of dicarboxylic acids and related compounds in aerosols from sapporo, japan:  
641 Implications for photochemical aging during long-range atmospheric transport. *J Geophys*  
642 *Res-Atmos* **2008**, *113* (D14).

643 [33] R. A. Duce, G. L. Hoffman, W. H. Zoller, Atmospheric trace-metals at remote northern  
644 and southern-hemisphere sites - pollution or natural. *Science* **1975**, *187* (4171), 59.

645 [34] X. Y. Zhang, S. L. Gong, Z. X. Shen, F. M. Mei, X. X. Xi, L. C. Liu, Z. J. Zhou, D.  
646 Wang, Y. Q. Wang, Y. Cheng, Characterization of soil dust aerosol in china and its transport  
647 and distribution during 2001 ace-asia: 1. Network observations. *J Geophys Res-Atmos* **2003**,  
648 *108* (D9).

649 [35] T. S. Bates, J. A. Calhoun, P. K. Quinn, Variations in the methanesulfonate to sulfate  
650 molar ratio in submicrometer marine aerosol-particles over the south-pacific ocean. *J*  
651 *Geophys Res-Atmos* **1992**, *97* (D9), 9859.

652 [36] C. M. Geng, Y. J. Mu, Carbonyl sulfide and dimethyl sulfide exchange between trees  
653 and the atmosphere. *Atmos Environ* **2006**, *40* (7), 1373.

654 [37] Z. G. Yi, X. M. Wang, M. G. Ouyang, D. Q. Zhang, G. Y. Zhou, Air-soil exchange of  
655 dimethyl sulfide, carbon disulfide, and dimethyl disulfide in three subtropical forests in south  
656 china. *J Geophys Res-Atmos* **2010**, *115*.

657 [38] J. J. Schauer, M. J. Kleeman, G. R. Cass, B. R. T. Simoneit, Measurement of emissions  
658 from air pollution sources. 5. C<sub>1</sub>-C<sub>32</sub> organic compounds from gasoline-powered motor  
659 vehicles. *Environ. Sci. Technol.* **2002**, *36* (6), 1169.

660 [39] Q. Zhang, D. G. Streets, G. R. Carmichael, K. B. He, H. Huo, A. Kannari, Z. Klimont, I.  
661 S. Park, S. Reddy, J. S. Fu, D. Chen, L. Duan, Y. Lei, L. T. Wang, Z. L. Yao, Asian  
662 emissions in 2006 for the nasa intex-b mission. *Atmos Chem Phys* **2009**, *9* (14), 5131.

663 [40] G. P. Yang, H. H. Zhang, L. P. Su, L. M. Zhou, Biogenic emission of dimethylsulfide  
664 (dms) from the north yellow sea, china and its contribution to sulfate in aerosol during  
665 summer. *Atmos Environ* **2009**, *43* (13), 2196.

666 [41] H. Mukai, Y. Yokouchi, M. Suzuki, Seasonal-variation of methanesulfonic-acid in the  
667 atmosphere over the oki islands in the sea of japan. *Atmos Environ* **1995**, *29* (14), 1637.

668 [42] J. M. Prospero, D. L. Savoie, R. Arimoto, Long-term record of nss-sulfate and nitrate in  
669 aerosols on midway island, 1981-2000: Evidence of increased (now decreasing?)  
670 anthropogenic emissions from asia. *J Geophys Res-Atmos* **2003**, *108* (D1).

671 [43] Y. Miyazaki, P. Q. Fu, K. Kawamura, Y. Mizoguchi, K. Yamanoi, Seasonal variations  
672 of stable carbon isotopic composition and biogenic tracer compounds of water-soluble  
673 organic aerosols in a deciduous forest. *Atmos Chem Phys* **2012**, *12* (3), 1367.

674 [44] E. P. Burford, M. Fomina, G. M. Gadd, Fungal involvement in bioweathering and  
675 biotransformation of rocks and minerals. *Mineral Mag* **2003**, *67* (6), 1127.

676 [45] Z. Q. Liu, Q. H. Liu, H. C. Lin, C. S. Schwartz, Y. H. Lee, T. J. Wang,  
677 Three-dimensional variational assimilation of modis aerosol optical depth: Implementation  
678 and application to a dust storm over east asia. *J Geophys Res-Atmos* **2011**, *116*.

679 [46] F. Giorgi, Dry deposition velocities of atmospheric aerosols as inferred by applying a  
680 particle dry deposition parameterization to a general circulation model. *Tellus B* **1988**, 40 (1),  
681 23.

682 [47] M. O. Andreae, Soot carbon and excess fine potassium: Long-range transport of  
683 combustion-derived aerosols. *Science* **1983**, 220, 1148.

684 [48] O. Hertel, C. A. Skjoth, S. Reis, A. Bleeker, R. M. Harrison, J. N. Cape, D. Fowler, U.  
685 Skiba, D. Simpson, T. Jickells, M. Kulmala, S. Gyldenkaerne, L. L. Sorensen, J. W. Erisman,  
686 M. A. Sutton, Governing processes for reactive nitrogen compounds in the european  
687 atmosphere. *Biogeosciences* **2012**, 9 (12), 4921.

688 [49] L. Wouters, S. Hagedoren, I. Dierck, P. Artaxo, R. Vangrieken, Laser microprobe mass  
689 analysis of amazon basin aerosols. *Atmos Environ a-Gen* **1993**, 27 (5), 661.

690 [50] B. R. T. Simoneit, Biomass burning - a review of organic tracers for smoke from  
691 incomplete combustion. *Appl Geochem* **2002**, 17 (3), 129.

692 [51] D. Hoffmann, A. Tilgner, Y. Iinuma, H. Herrmann, Atmospheric stability of  
693 levoglucosan: A detailed laboratory and modeling study. *Environ Sci Technol* **2010**, 44 (2),  
694 694.

695 [52] J. M. Pacyna, E. G. Pacyna, An assessment of global and regional emissions of trace  
696 metals to the atmosphere from anthropogenic sources worldwide. *Environmental Reviews*  
697 **2001**, 9 (4), 269.

698 [53] S. Gilardoni, E. Vignati, F. Cavalli, J. P. Putaud, B. R. Larsen, M. Karl, K. Stenstrom, J.  
699 Genberg, S. Henne, F. Dentener, Better constraints on sources of carbonaceous aerosols using  
700 a combined c-14 - macro tracer analysis in a european rural background site. *Atmos Chem*  
701 *Phys* **2011**, 11 (12), 5685.

702 [54] P. Q. Fu, K. Kawamura, M. Kobayashi, B. R. T. Simoneit, Seasonal variations of sugars  
703 in atmospheric particulate matter from goson, jeju island: Significant contributions of  
704 airborne pollen and asian dust in spring. *Atmos Environ* **2012**, 55, 234.

705 [55] A. Lepsova, V. Mejstrik, Accumulation of trace-elements in the fruiting bodies of  
706 macrofungi in the krusnehoj mountains, czechoslovakia. *Sci Total Environ* **1988**, 76 (2-3),  
707 117.

708 [56] E. Polar, Zinc in pollen and its incorporation into seeds. *Planta* **1975**, 123 (1), 97.

709 [57] J. O. Nriagu, A global assessment of natural sources of atmospheric trace-metals. *Nature*  
710 **1989**, 338 (6210), 47.

711 [58] R. C. Henry, C. W. Lewis, P. K. Hopke, H. J. Williamson, Review of receptor model  
712 fundamentals. *Atmos Environ* **1984**, 18 (8), 1507.

- 713 [59] T. Pauliquevis, L. L. Lara, M. L. Antunes, P. Artaxo, Aerosol and precipitation  
714 chemistry measurements in a remote site in central amazonia: The role of biogenic  
715 contribution. *Atmos Chem Phys* **2012**, *12* (11), 4987.
- 716 [60] C. W. Liu, K. H. Lin, Y. M. Kuo, Application of factor analysis in the assessment of  
717 groundwater quality in a blackfoot disease area in taiwan. *Sci Total Environ* **2003**, *313* (1-3),  
718 77.
- 719 [61] R. C. MacCallum, K. F. Widaman, S. B. Zhang, S. H. Hong, Sample size in factor  
720 analysis. *Psychol Methods* **1999**, *4* (1), 84.
- 721
- 722

723 **Figure captions.**

724 **Fig. 1.** Seasonal variations of meteorological parameters (ambient temperature, RH, wind  
725 speed and precipitation) in Sapporo, northern Japan.

726 **Fig. 2.** Plots of 10-day backward air mass trajectories arriving in Sapporo at 500 m AGL.  
727 Color scale shows the altitude of the air parcel AGL.

728 **Fig. 3.** Temporal variations of (a) ionic species and (b) trace metals.

729 **Fig. 4.** Relative abundances of ionic species to total ionic mass in (a) autumn, (b) winter, (c)  
730 spring and (d) summer.

731 **Fig. 5.** Box-and-whisker plots of (a)  $\text{MS}^-$  and  $\text{SO}_4^{2-}$  and (b)  $\text{Na}^+$  and  $\text{Mg}^{2+}$  in autumn, winter,  
732 spring and summer. Lower and upper ends of the box show the quartiles at 25% and 75%  
733 whereas upper and lower bars of the whiskers present the quartiles at 10% and 90%. The  
734 cross bar in the box shows the median. Open circles mean outliers ( $1.25 \times$  interquartile  
735 distance).

736 **Fig. 6.** Temporal variations of concentrations of tracer species. Plant wax alkanes, fatty acids  
737 and fatty alcohols are sums of  $\text{C}_{23}$  to  $\text{C}_{37}$ ,  $\text{C}_{12}$ - $\text{C}_{32}$  and  $\text{C}_{18}$ - $\text{C}_{32}$  compounds, respectively.  
738 Isoprene derived compounds are sums of 2-methylglyceric acid,  
739 cis-2-methyl-1,3,4-trihydroxy-1-butene, 3-methyl-2,3,4-trihydroxy-1-butene  
740 trans-2-methyl-1,3,4-trihydroxy-1-butene, 2-methylthreitol and 2-methylerythritol whereas  
741  $\alpha$ -pinene derived compounds are sums of 3-hydroxyglutaric, pinonic, pinic and  
742 3-methyl-1,2,3-butanetricarboxylic acids. The data are from Pavuluri et al.

743 **Fig. 7.** Scatter plots of the concentrations of Ni, Cu and As as a function of the concentrations  
744 of mannitol. The data of mannitol are from Pavuluri et al.<sup>[25]</sup>

745 **Table 1.** Statistical summary for the concentrations ( $\text{ng m}^{-3}$ ) of methanesulfonate, major  
 746 inorganic ions and trace metals in atmospheric aerosol (TSP) samples ( $n = 21$ ) collected from  
 747 Sapporo, northern Japan during September 2, 2009 to October 5, 2010.

	Range	Median/Average	Standard Deviation
<i>Ionic species</i>			
MS <sup>-</sup>	15.6–83.4	34.8/40.6	20.8
Cl <sup>-</sup>	12.0–3850	929/1290	1250
NO <sub>3</sub> <sup>-</sup>	183–2670	1248/1200	728
SO <sub>4</sub> <sup>2-</sup>	1556–5710	3494/3470	1030
Na <sup>+</sup>	294–2140	933/1070	547
NH <sub>4</sub> <sup>+</sup>	68.8–1260	78.1/68.6	42.3
K <sup>+</sup>	94.5–233	139/144	40.6
Ca <sup>2+</sup>	139–1564	471/507	295
Mg <sup>2+</sup>	57.5–299	128/152	68.1
<i>Trace metals</i>			
Al	64.8–1830	475/532	372
Ca	196–2920	938/1070	578
Ti	4.03–82.8	30.6/31.7	16.3
V	0.39–9.40	3.15/3.42	2.12
Cr	0.18–4.35	2.41/2.36	0.88
Mn	3.61–51.8	19.8/19.9	10.3
Fe	40.7–1990	652/684	406
Ni	2.36–18.5	11.4/11.4	3.77
Cu	1.95–18.9	9.88/11.0	4.20
Zn	21.8–189	57.1/66.3	34.0
As	0.74–3.80	2.41/2.44	0.80
Cd	0.074–0.43	0.19/0.22	0.10
Pb	3.56–19.0	9.74/10.8	4.47

748



749 **Table 2.** Varimax rotated factor loadings for ionic species in the Sapporo TSP samples ( $n =$   
 750 21) during the campaign<sup>a</sup>.

Variable	Factor			Communality
	F1	F2	F3	
MS <sup>-</sup>	-0.13	<b>0.91</b>	-0.09	0.85
Cl <sup>-</sup>	0.46	-0.63	0.49	0.85
NO <sub>3</sub> <sup>-</sup>	0.18	-0.32	<b>0.77</b>	0.72
SO <sub>4</sub> <sup>2-</sup>	-0.13	<b>0.89</b>	0.34	0.92
Na <sup>+</sup>	<b>0.79</b>	-0.55	0.18	0.96
NH <sub>4</sub> <sup>+</sup>	-0.76	0.16	<b>0.60</b>	0.96
K <sup>+</sup>	0.14	0.24	<b>0.81</b>	0.73
Ca <sup>2+</sup>	<b>0.67</b>	0.37	0.48	0.82
Mg <sup>2+</sup>	<b>0.91</b>	-0.28	0.28	0.98
Eigenvalue	4.04	2.38	1.38	
% of Variance	31	30	26	
Source type	Natural	Photochemical	Biomass burning & Anthropogenic	

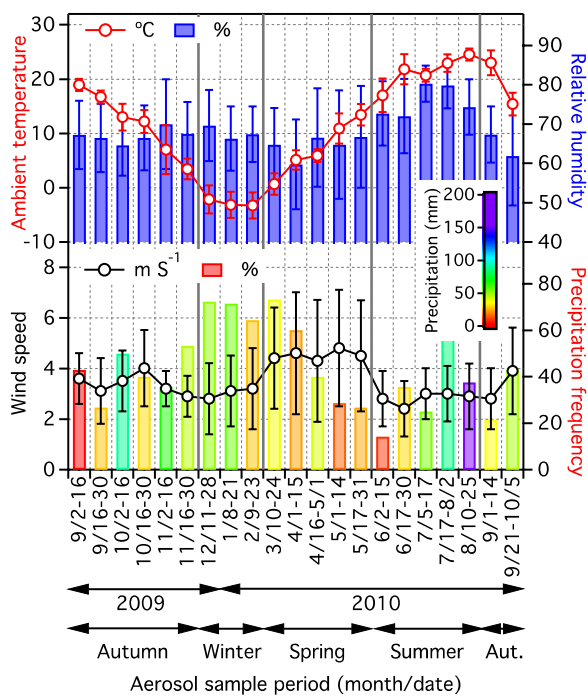
751 <sup>a</sup>Factor loadings  $\geq 0.5$  are in bold.

752 **Table 3.** Varimax rotated factor loadings for trace metals in the Sapporo TSP samples ( $n = 21$ )  
 753 during the campaign<sup>a</sup>.

Variable	Factor			Communality
	F1	F2	F3	
Al	<b>0.97</b>	0.18	0.03	0.97
Ca	<b>0.92</b>	0.26	0.07	0.92
Ti	<b>0.94</b>	0.23	0.07	0.95
V	0.43	<b>0.58</b>	-0.07	0.52
Cr	<b>0.72</b>	0.08	0.40	0.68
Mn	<b>0.93</b>	0.20	0.26	0.97
Fe	<b>0.96</b>	0.18	0.17	0.99
Ni	0.24	<b>0.83</b>	-0.24	0.81
Cu	0.06	<b>0.87</b>	0.27	0.84
Zn	0.11	0.47	<b>0.52</b>	0.51
As	0.26	<b>0.71</b>	0.42	0.74
Cd	0.12	-0.08	<b>0.96</b>	0.94
Pb	0.21	0.14	<b>0.92</b>	0.92
Eigenvalue	6.81	2.14	1.81	
% of Variance	41	21	20	
Source type	Soil dust	Industrial	Fossil fuel combustion & road dust	

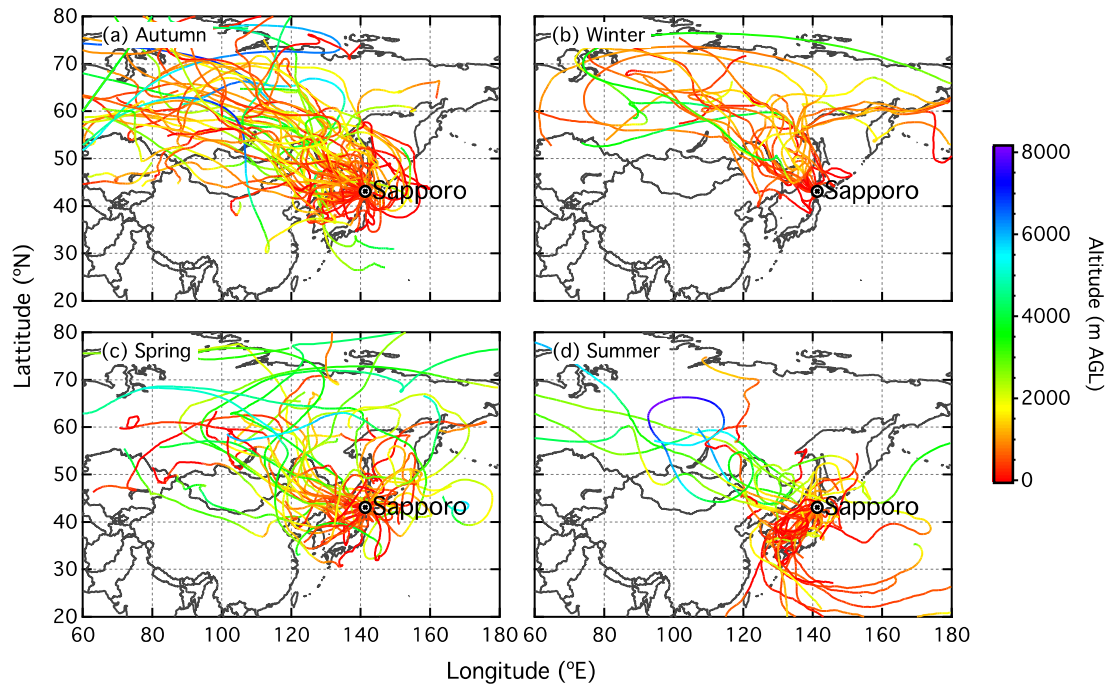
754 <sup>a</sup>Factor loadings  $\geq 0.5$  are in bold.

755 **Fig. 1.**

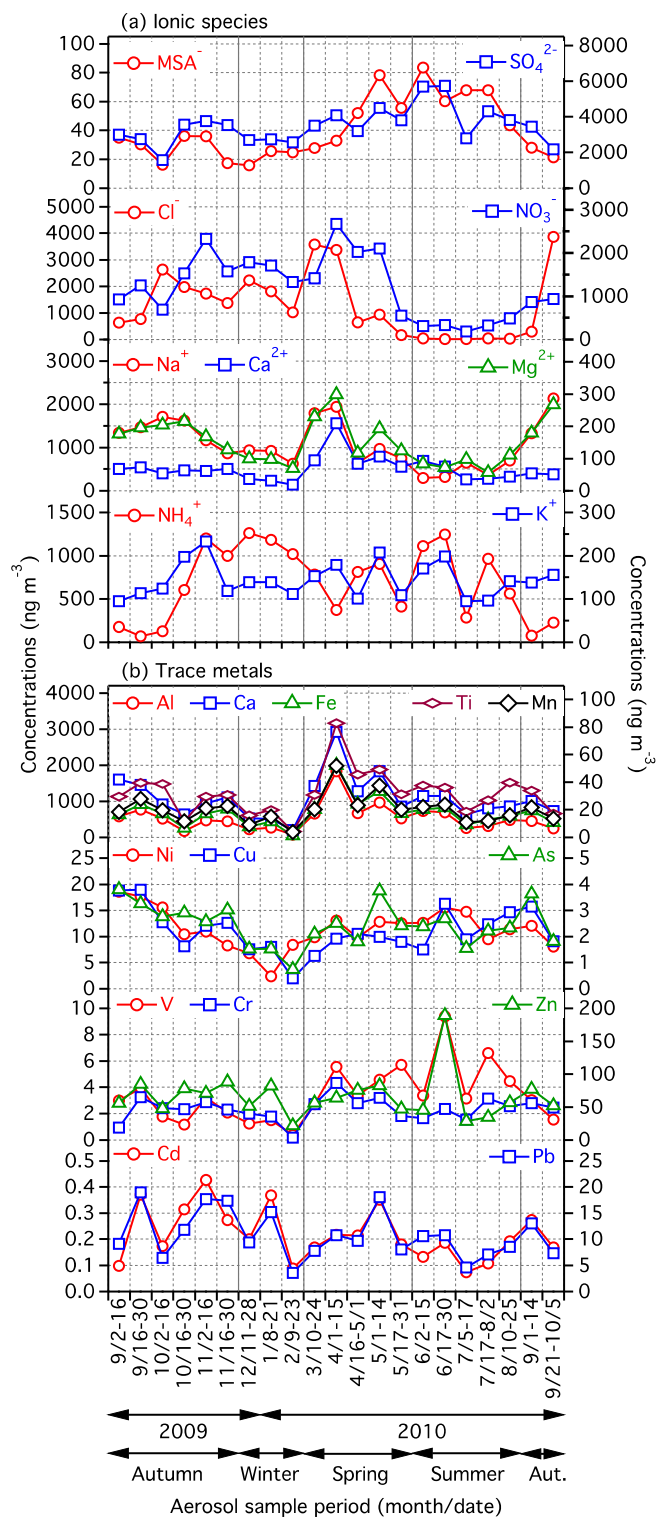


756

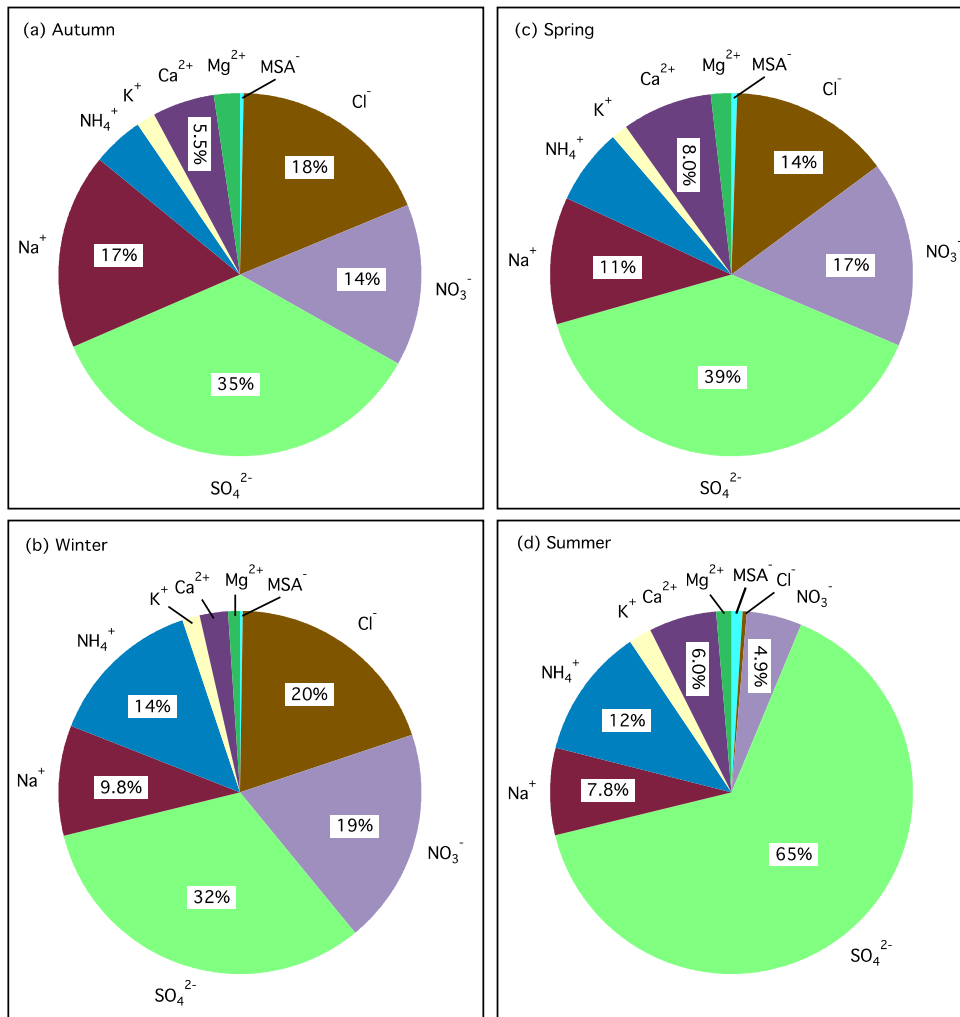
757 **Fig. 2.**



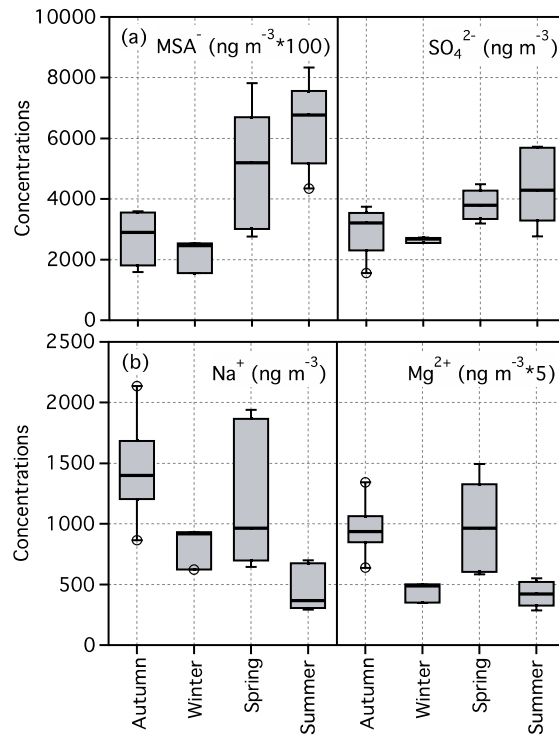
758



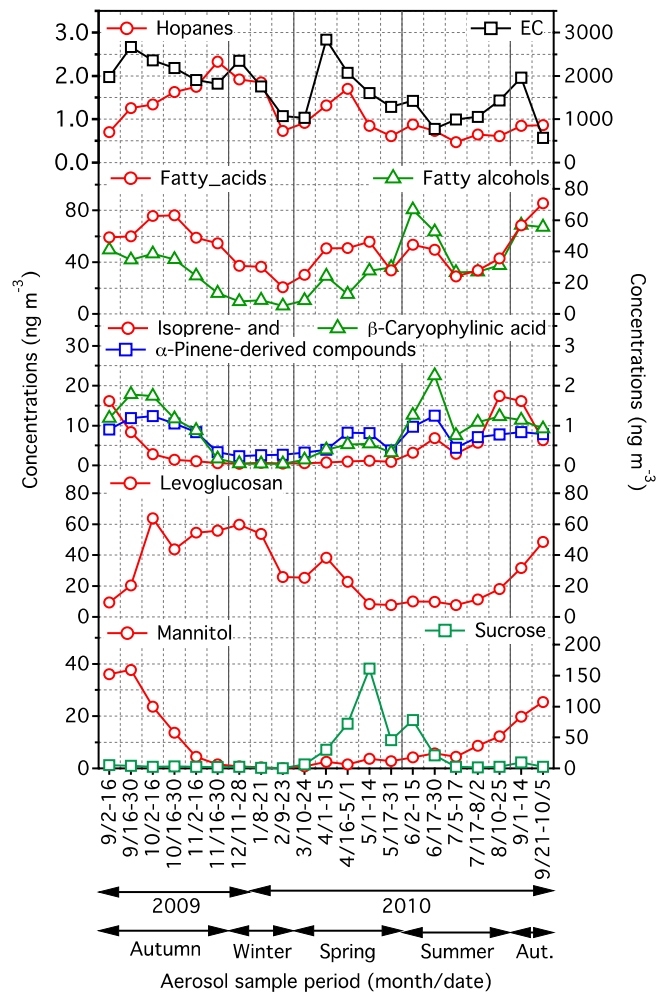
761 **Fig. 4.**



762



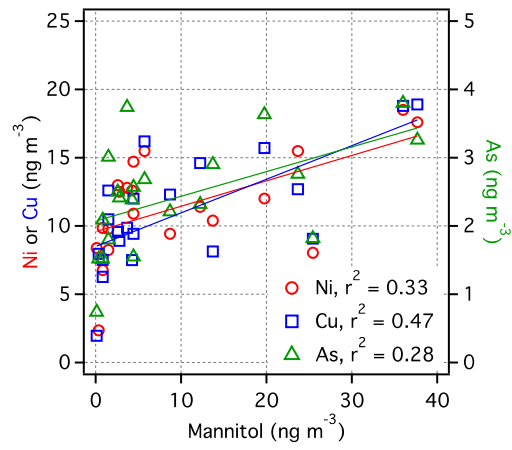
765 **Fig. 6.**



766



767 **Fig. 7.**



768